Flow resistance in skimming flows in stepped spillways and its modelling

H. Chanson, Y. Yasuda, and I. Ohtsu

Abstract: Dams and weirs must be equipped with adequate flood-release facilities for a safe dissipation of the kinetic energy of the flow. With stepped spillway design, it is essential to accurately predict the flow-resistance contribution of the steps. The authors investigate the flow resistance of skimming flows and associated form losses. Recent laboratory experiments were systematically performed with channel slopes ranging from 5.7° up to 55° and the results are compared with existing laboratory and prototype data. The results provide a better understanding of the basic flow patterns and flow-resistance mechanisms and emphasize that form loss is dominant. Simple analytical models provide a reasonable order of magnitude of the pseudo-boundary shear stress and the recirculation cavity ejection frequency. Altogether, more than 38 model studies and four prototype investigations (for a total of more than 700 data points) are reanalysed.

Key words: stepped spillway, flow resistance, skimming flow, form drag, physical and analytical modelling.

Résumé : Les barrages et ouvrages de retenues d'eau doivent être équippés de systèmes d'évacuations des eaux de crues, permettant une dissipation efficace de l'énergie cinétique de l'écoulement. Dans le cas d'évacuateurs de crues en marches d'escalier, il est particulièrement important d'estimer correctement les forces de frottement dues aux marches. On étudie, particulièrement, la résistance de frottement des écoulements extrèmement turbulents « skimming flows » et leur résistance de forme. Des essais en laboratoires ont été conduits systématiquement pour des pentes comprises entre 5,7 et 55 degrés, et les données expérimentales sont comparées avec des études antérieures. Les résultats permettent de comprendre mieux les caractéristiques des écoulements et les mécanismes de base de perte de charge. Ils démontrent, en particulier, l'importance de la résistance de forme « form drag ». On présente, de plus, de simples modèles analytiques fournissant une estimation raisonnable de la contrainte équivalente de paroi « pseudo-boundary shear stress » et de la fréquence d'éjection des zones de recirculation. Au total, plus de 38 études en laboratoire et 4 études sur prototypes (regroupant plus de 700 points de mesure) sont ré-analysées.

Mots clés : évacuateur de crues en marches d'escalier, perte de charge, écoulement extrèmement turbulent, résistance de forme, modèlisation physique et analytique.

Introduction

During large rainfall events, flood waters rush through, above, and beside man-made dams. Significant damage may occur if the energy of the flow, especially its kinetic energy, is not dissipated safely. One type of flood-release facility is the stepped spillway. It is characterized by significant flow resistance and associated energy dissipation caused by the steps. The design yields smaller, more economical dissipation structures at the downstream end of the chute. The world's oldest stepped spillway is presumably the overflow stepped weir in Akarnania, Greece, built around 1300 B.C. The weir, 10.5 m high with a 25 m long crest, was equipped with a stepped overflow (Knauss 1995; Chanson 2000). The downstream slope is stepped (14 steps) with masonry rubble set in mortar. The mean slope is about 45°, varying from 39° to 73°, and the step height ranges from 0.6 to 0.9 m. The stepped weir was used for several centuries. It is still standing and flash floods spill over the stepped chute.

The recent regain of interest in stepped spillways has been associated with the development of new construction materials (e.g., roller-compacted concrete) and design techniques (e.g., overflow protection systems for embankments) (e.g., Chanson 1995; Ohtsu and Yasuda 1998). Although modern roller-compacted concrete (RCC) stepped spillways are designed for a skimming flow regime (Fig. 1), there is some controversy on an accurate estimate of the flow resistance. Model and prototype data exhibit little correlation, with flow-resistance data scattered over three orders of magnitude (e.g., Ohtsu and Yasuda 1998; Chanson et al. 2000) (Fig. 2).

In the present paper, the authors investigate the flow resistance in skimming flows. New experiments were performed systematically with channel slopes ranging from 5.7° to 55°. Basic flow patterns are presented and the experimental results are compared with existing data, i.e., over 38 model and four prototype studies are reanalysed, including more

Received 11 April 2002. Revision accepted 4 September 2002. Published on the NRC Research Press Web site at http://cjce.nrc.ca on 29 October 2002.

H. Chanson.[1] Department of Civil Engineering, The University of Queensland, Brisbane QLD 4072, Australia. **Y. Yasuda and I. Ohtsu.** Department of Civil Engineering, College of Science and Technology, Nihon University, Tokyo 101-8303, Japan.

Written discussion of this article is welcomed and will be received by the Editor until 30 April 2003.

[1]Corresponding author (e-mail: h.chanson@mailbox.uq.edu.au).

 DOI: 10.1139/L02-083

Fig. 1. Definition sketch of skimming flow.

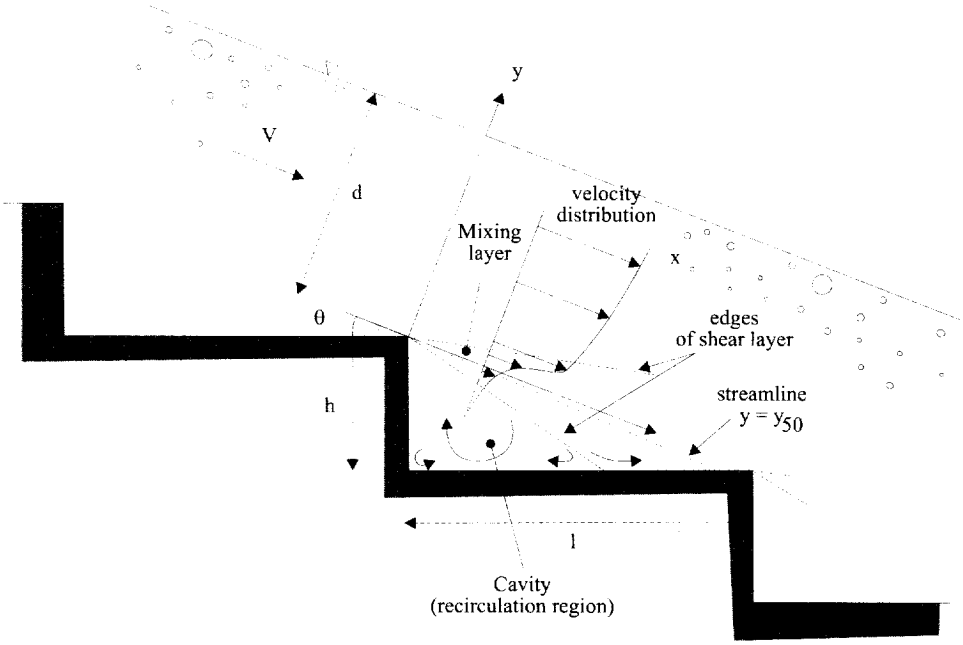

Fig. 2. Darcy friction factor of skimming flows on steep stepped chute (θ > 20°) (455 laboratory data points).

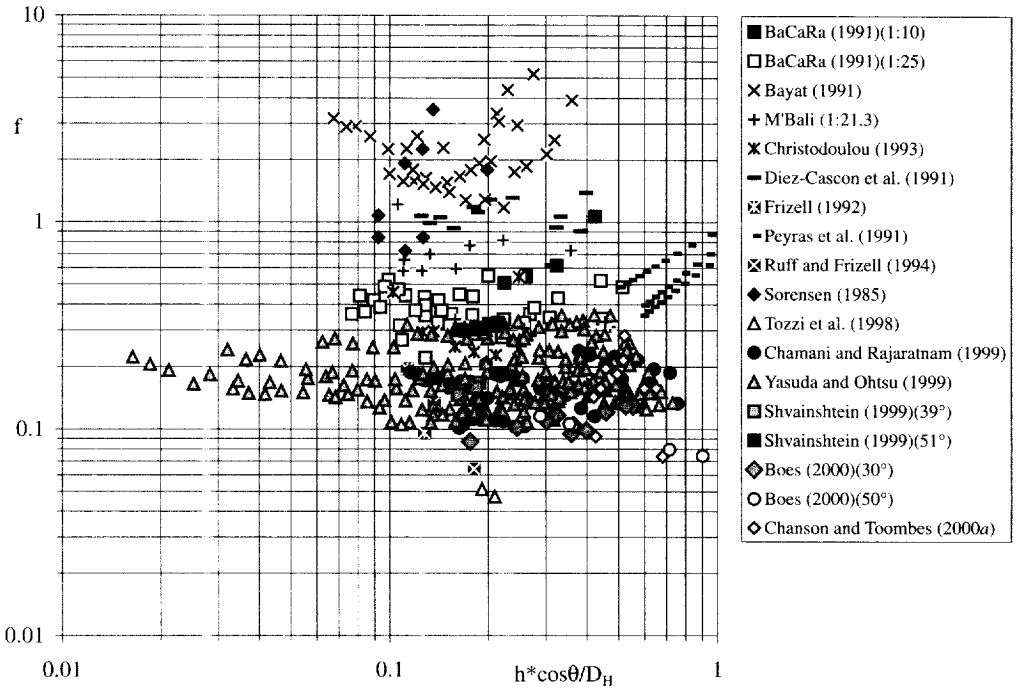

than 700 data points. The purpose of this paper is to assess critically the overall state of this field and present new conclusions valid for both flat (channel slope θ < 20°) and steep (θ > 20°) spillways with skimming flows.

Basic equations

Although the flow resistance on smooth-invert chutes is primarily due to skin friction, skimming flows over stepped chutes are characterized by significant form losses. The water skims over the step edges with formation of recirculating vortices between the main flow and the step corners (Fig. 1). In *uniform equilibrium flows*, the momentum principle states that the boundary friction force exactly equals the gravity force component in the flow direction, i.e., the weight of water component acting parallel to the pseudo-bottom formed by the step edges. It yields

$$[1] \qquad \tau_o P_w = \rho_w g A_w \sin\theta$$

where τ_o is the average shear stress between the skimming flow and the recirculating fluid underneath, P_w is the wetted

perimeter, ρ_w is the water density, g is the gravity constant, A_w is the water flow cross-sectional area, and θ is the mean bed inclination angle. For a wide channel, eq. [1] becomes

$$[2] \quad \tau_o = \left[\int_{y=0}^{y=Y_{90}} \rho_w (1-C)\, dy \right] g \sin\theta$$

where C is the void fraction, also called air concentration, and is defined as the volume of air per unit volume of air and water; and Y_{90} is the distance normal to the pseudo-bottom where $C = 90\%$.

Kazemipour and Apelt (1983) stressed that to try to account for the form losses with a Gauckler-Manning or Darcy-Weisbach formula is unsatisfactory. Nevertheless, the Darcy-Weisbach formula is used for this study of skimming flows because it facilitates a comparison between smooth-invert and stepped chute flows. Further, the drag coefficient of uniformly spaced roughness (e.g., steps) is proportional to the Darcy coefficient (Schlichting 1979). By analogy with clear-water, open-channel flows, the average boundary shear stress may be expressed in terms of the Darcy friction factor as

$$[3] \quad \tau_o = \frac{f_e}{8} \rho_w V^2$$

where f_e is the Darcy friction factor of the air–water flow, and V is the mean flow velocity (or equivalent clear-water flow velocity). By continuity, V equals

$$[4] \quad V = \frac{q_w}{\int_{y=0}^{y=Y_{90}} (1-C)\, dy}$$

where q_w is the water discharge per unit width.

In dimensionless terms, the momentum equation at uniform equilibrium in a wide channel yields

$$[5] \quad \frac{\tau_o}{(1/8)\rho_w V^2} = \frac{8g}{q_w^2} \left[\int_{y=0}^{y=Y_{90}} (1-C)\, dy \right]^3 \sin\theta$$

In *gradually varied flows*, the friction factor must be deduced from the friction slope S_f, which is the slope of the total head line (Henderson 1966; Chanson 1999). For a wide channel, it yields

$$[6] \quad \frac{\tau_o}{(1/8)\rho_w V^2} = \frac{8g}{q_w^2} \left[\int_{y=0}^{y=Y_{90}} (1-C)\, dy \right]^3 S_f$$

Free-surface aeration is always substantial in prototype skimming flows and its effects must not be neglected. Downstream of the inception point of free-surface aeration, the distribution of air concentration may be described by a diffusion model:

$$[7] \quad C = 1 - \tanh^2\left(K' - \frac{y}{2D' Y_{90}} \right)$$

where tanh is the hyperbolic tangent function, y is the distance normal to the pseudo-bottom formed by the step edges, D' is the dimensionless turbulent diffusivity, and K' is an integration constant (Chanson 1997). D' and K' are functions of the mean air content C_{mean} only and can be estimated as

$$[8] \quad D' = \frac{0.848 C_{mean} - 0.00302}{1 + 1.1375 C_{mean} - 2.2925 C_{mean}^2}$$

$$[9] \quad K' = \tanh^{-1}(\sqrt{0.1}) + \frac{0.5}{D'}$$

for $C_{mean} < 0.7$. Equation [7] compares favourably with stepped chute data obtained in models and prototypes (Baker 1994; Ruff and Frizell 1994; Chamani and Rajaratnam 1999; Matos et al. 1999; Chanson and Toombes 2001*a*) (Fig. 3).

Flow resistance in skimming flows

Recent laboratory studies of stepped channels provided significant contributions to the understanding of stepped channel flows (e.g., BaCaRa 1991; Ohtsu and Yasuda 1997). Dynamic similarity of skimming flows is, however, complex because of the role of the steps in enhancing turbulent dissipation and free-surface aeration. For uniform equilibrium flows (i.e., normal flows) down a prismatic rectangular channel with horizontal steps, a dominant flow feature is the momentum exchange between the free stream and the cavity flow within the steps (Fig. 1). A complete dimensional analysis yields

$$[10] \quad F\left(\frac{V}{\sqrt{gd}}; \rho_w \frac{Vd}{\mu_w}; \frac{g\mu_w^4}{\rho_w \sigma^3}; C_{mean}; \frac{d}{h}; \frac{W}{h}; \theta; \frac{k_s'}{h} \right) = 0$$

where V and d are the mean flow velocity and flow depth, respectively, at uniform equilibrium flow conditions; W is the channel width; h is the step height; k_s' is the skin roughness height; g is the gravity acceleration; μ_w and ρ_w are the dynamic viscosity and density of water, respectively; and σ is the surface tension. For air–water flows, the equivalent clear-water depth is defined as

$$[11] \quad d = \int_{y=0}^{y=Y_{90}} (1-C)\, dy$$

From left to right, the dimensionless terms in eq. [10] are the Froude number, the Reynolds number, the Morton number, the amount of entrained air, and four terms that characterize the cavity shape and skin-friction effects on the cavity walls.

Equation [10] illustrates that a Froude similitude with geometric similarity and the same fluids in model and prototype does not describe the complexity of stepped spillway flows. BaCaRa (1991) described a systematic laboratory investigation of the M'Bali Dam spillway with model scales of 1/10, 1/21.3, 1/25, and 1/42.7. For the scales 1/25 and 1/42.7, the flow resistance was improperly reproduced with a Froude similitude. Further studies demonstrated that air entrainment is poorly reproduced on small-size models (Kobus 1984; Chanson 1997). Chanson (1997, p. 236) rec-

Fig. 3. Void fraction distributions in stepped chute flows: comparison with eq. [7].

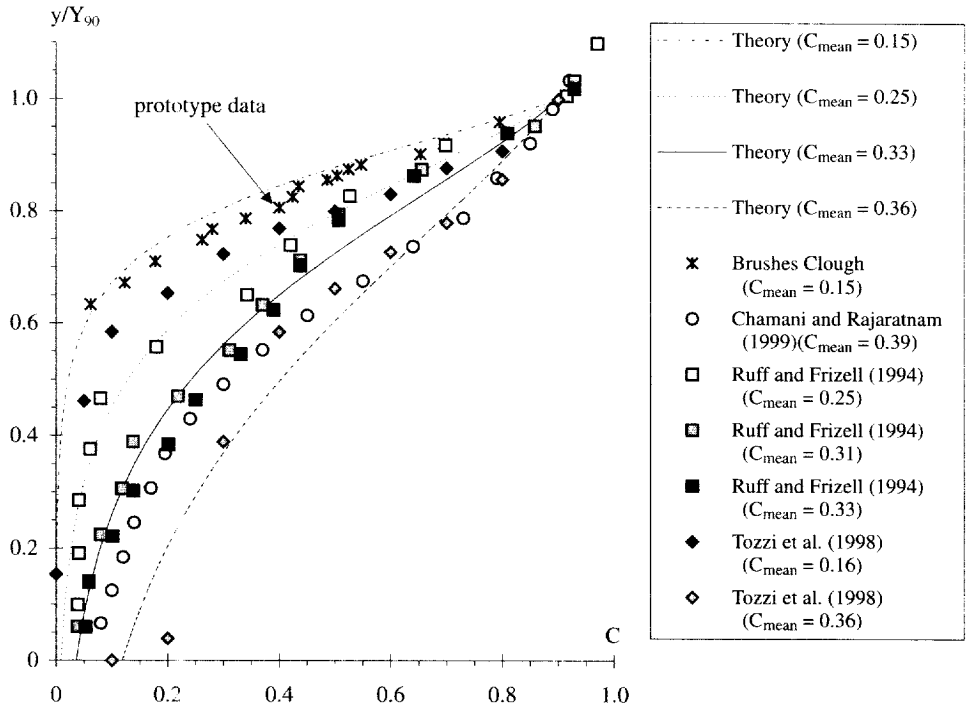

ommended the use of model scales ranging from 1/1 to 1/10 to avoid significant scale effects.

New experimental study

A systematic study of stepped spillway flows was undertaken at Nihon University (Yasuda and Ohtsu 1999). Experiments were performed in four 0.4 m wide stepped channels with bottom slopes of 5.7°, 11.3°, 19°, 30°, and 55°, step heights ranging from 0.002 to 0.08 m, and flow rates per unit width of between 0.008 and 0.08 m^2/s. Each channel was followed by a horizontal stilling basin. Clear-water depths were recorded with a point gauge. Pressure and velocity in clear-water flows were measured with a Pitot tube. Void fractions were recorded with an optical fibre probe (single tip). The skimming flow depth was measured by two methods, the clear-water flow depth deduced from void-fraction profiles (eq. [11]) and an indirect method based on the water depth measurement in the stilling basin. In the stilling basin, the momentum equation across the jump yields

$$[12] \quad \rho_w q_w (V_2 - V_1) = \frac{1}{2} P_{bottom} d_1 - \frac{1}{2} \rho_w g d_2^2$$

where P_{bottom} is the invert pressure upstream of the hydraulic jump; d_1 and V_1 are the supercritical flow depth and velocity, respectively, upstream of the hydraulic jump; and d_2 and V_2 are the flow depth and velocity, respectively, downstream of the hydraulic jump. At the chute toe, the energy equation implies that the residual head equals

$$[13] \quad H_{res} = d \cos\theta + \frac{V^2}{2g} = C_P d_1 + \frac{V_1^2}{2g}$$

where d and V are the flow depth and velocity, respectively, at the end of the stepped chute; and C_P is a pressure correction coefficient defined as

$$C_P = \frac{1}{\rho_w g q_w d_1} \int_{y=0}^{y=d_1} (P + \rho_w g y) v \, dy$$

where P is the pressure. Pressure and velocity distributions upstream of the jump were measured in situ with Pitot tube and pressure tappings. The data showed that C_P was significantly larger than unity. Comparison between clear-water flow depths deduced from the optical fibre probe (eq. [11]) and indirect supercritical depth (eq. [13]) showed agreement between the two methods within 10% and no significant trends between results of clear-water depths obtained by the different methods.

Additional experiments were conducted for two intermediate slopes (θ = 16° and 22°) and large step heights (h = 0.1 m and 0.05 m) at the University of Queensland (Chanson and Toombes 2001*a*). This study was focused on the basic air–water flow properties and cavity recirculation processes.

Data analysis

The experimental data were analysed using eqs. [2] and [5] for uniform equilibrium flows and eq. [6] for gradually varied flows. The data are compared with those from the reanalysis of over 40 model and prototype studies using the same equations. Some studies conducted detailed air–water flow measurements (e.g., void fraction distributions), while others attempted to record a pseudo-water depth (Table 1). Results derived from air–water flow data provide genuine estimates of the dimensionless boundary shear stress, herein denoted f_e. Estimates derived from eq. [13] are denoted f_p. Results based on pseudo-water depth give a rough, less accurate estimate that is denoted f_w.

The combined analysis (over 700 data points) shows that the flow resistance is larger on stepped chutes than on smooth channels, but the steep stepped chute data show very little correlation (Fig. 2). The study further highlights the

Table 1. Reanalysed experimental data of flow resistance in skimming flows.

Reference	θ (°)	h (m)	W (m)	Remarks
Estimates based on results derived from air–water flow data (f_e)				
Baker 1994	18.4	0.19		Brushes Clough dam spillway; inclined downwards steps; trapezoidal channel
Ruff and Frizell 1994	26.6	0.154	1.52	Inclined downwards steps
Chamani and Rajaratnam 1999	51.3	0.313; 0.125	0.3	
	59	0.313–0.125	0.3	
Ohtsu et al. 2000	55	0.025	0.4	
Matos 2000	53.1	0.08	1.0	
Boes 2000	30	0.046; 0.092	0.5	
	50	0.031; 0.093	0.5	
Chanson and Toombes 2001*a*	15.9	0.05; 0.10	1.0	
	21.8	0.10	1.0	
Estimates from results based on pseudo-water depth (f_w)				
Grinchuk et al. 1977	8.7	0.41	14.2	Dneiper power plant
BaCaRa 1991	53.1	0.06	1.5	
	53.1	0.024		
	59	0.024		
	63.4	0.024		
Bayat 1991	51.3	0.02–0.03	0.3	
Bindo et al. 1993	51.3	0.019; 0.038	0.9	
Christodoulou 1993	55	0.025	0.5	
Diez-Cascon et al. 1991	53.1	0.03; 0.06	0.8	
Frizell 1992	26.6	0.051	0.457	Inclined downwards steps
Peyras et al. 1991	18.4; 26.6; 45	0.02	0.8	Gabion models
Shvajnshtein 1999	38.7	0.05	0.48	
	51.3	0.0625	0.48	
Sorensen 1985	52	0.0024; 0.061	0.305	
Estimates derived from eq. [13] (f_p)				
Yasuda and Ohtsu 1999	5.7	0.006–0.010	0.4	
	11.3	0.006–0.10	0.4	
	19	0.002–0.08	0.4	
	30	0.004–0.07	0.4	
	55	0.003–0.064	0.4	

lack of uniformity in the experimental procedure and data processing. Many studies gave incomplete experimental information with uncertainties of up to 200%.

A conditional analysis was applied. Only the following data were retained: prototype data, large-size model data (h > 0.020 m, Reynolds number Re > 1 × 10^5), and model studies published after January 1997. This analysis gives a greater statistical weight to prototype data and recent works. Basic results of the conditional analysis indicate different trends for flat and steep chutes (Figs. 4*a* and 4*b*).

For flat chutes (θ < 20°), prototype data obtained with horizontal and downward-inclined steps exhibit higher flow resistance than laboratory data:

$$[14a] \quad \frac{1}{\sqrt{f}} = -1.224 - 1.245 \ln\left(\frac{h \cos\theta}{D_H}\right)$$

for prototype flat chutes

$$[14b] \quad \frac{1}{\sqrt{f_p}} = -2.430 - 0.2676 \ln\left(\frac{h \cos\theta}{D_H}\right)$$

for model flat chutes

with normalized correlation coefficients of 0.9525 (10 data points) and 0.4872 (52 data points), respectively, where f is the Darcy friction factor, f_p is the Darcy friction factor calculated using eq. [13], and D_H is the hydraulic diameter. By comparison, the Colebrook-White formula for flat rough walls is

$$[15] \quad \frac{1}{\sqrt{f}} = -1.14 - 4.605 \ln\left(\frac{k_s'}{D_H}\right)$$

Equation [15] is compared with data and eqs. [14*a*] and [14*b*] in Fig. 4*a*.

For steep chutes (θ > 20°), the friction factor data present no obvious correlation with the relative step roughness height $h \cos\theta/D_H$ and the Reynolds, Froude, and Weber numbers (Fig. 4*b*). The data appear to be distributed around three dominant values: $f \approx 0.105$, 0.17, and 0.30 (166 data points), as shown in Fig. 4*c*.

Discussion

Cavity recirculation and ejection mechanisms

Skimming flows are characterized by unsteady momen-

Fig. 4. Flow resistance in skimming flow: conditional analysis. (*a*) Flat stepped chute data ($\theta < 20°$) (62 data points). Comparison with eqs. [14*a*] and [14*b*]. (*b*) Steep stepped chute data ($\theta > 20°$) (166 data points). Comparison with eq. [17]. (*c*) Probability distribution function (Pdf) of steep chute friction factor ($\theta > 20°$) (166 data points).

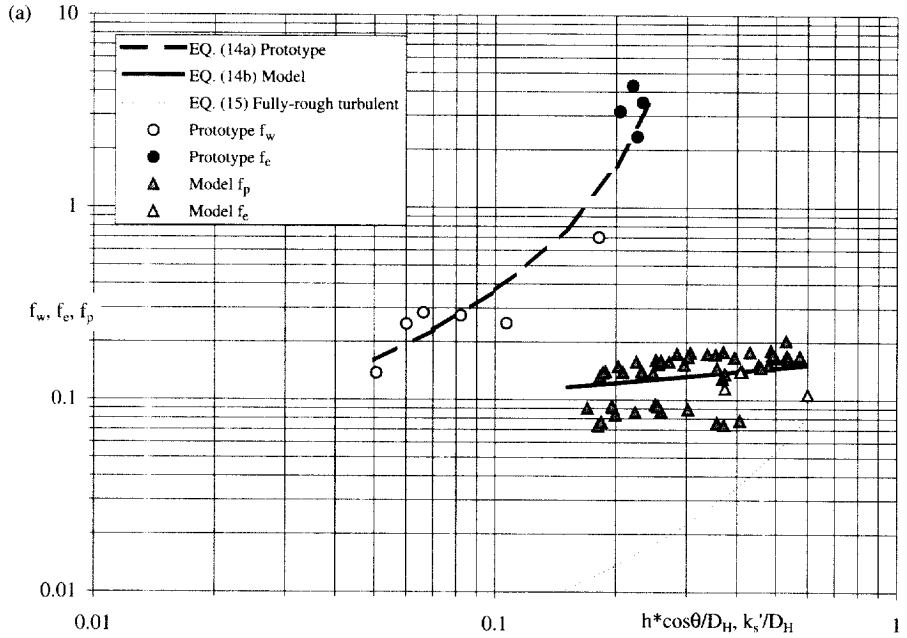

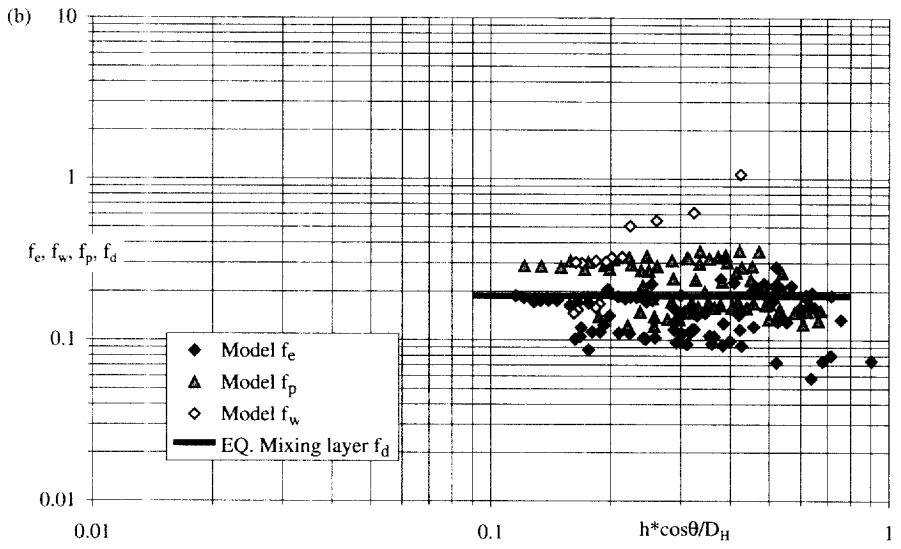

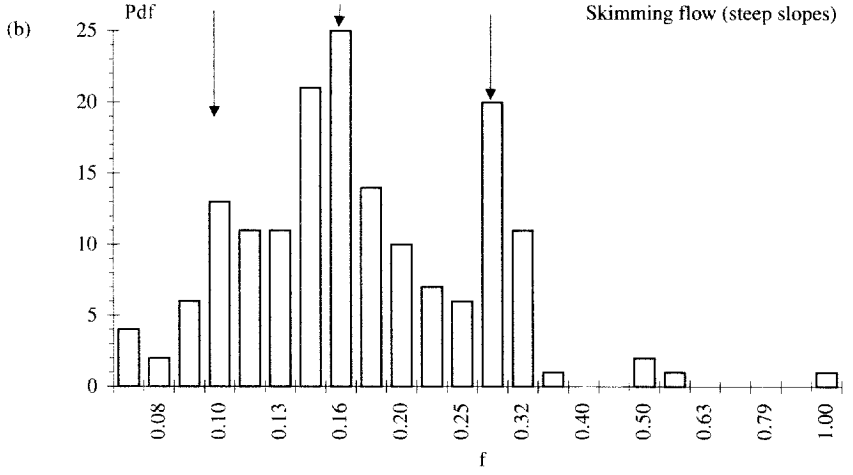

tum exchanges between the main stream and cavity flows. The recirculating fluid will, at irregular time intervals, be swept away (i.e., flow outward) into the main flow and replaced by fresh fluid. The ejection mechanism appears sequential. Once one cavity outflow occurs, it induces a sequence of outflows at the downstream cavities. The sequential process is illustrated in Fig. 5. The sequential ejection process extends down the entire slope. It was observed visually for all investigated slopes by Yasuda and Ohtsu (1999) and Chanson and Toombes (2001*a*), but the sequential mechanism seemed more frequent on the steep chute geometries. A similar pattern was documented with skimming flows past strip roughness (rectangular cavity: Djenidi et al. 1994; Elavarasan et al. 1995; triangular cavity: Tantirige et al. 1994), and the sequential fluid ejection process was observed on the M'Bali Dam stepped spillway model by A. Lejeune (personal communication).

Cavity recirculation is very energetic and contributes significantly to the form drag. Turbulent motion in the step cavity induces viscous dissipation while irregular fluid exchanges with the free stream maintain the recirculation process. Energy considerations provide a relationship between cavity ejection frequency, form drag, and energy dissipation.

At uniform equilibrium, the rate of energy loss between two adjacent step edges equals $\rho_w Q_w h$ where Q_w is the water discharge, whereas the energy is dissipated in the recirculation cavity at a rate proportional to the ejection frequency F_{ej}, the volume of ejected fluid, and the main flow velocity V. The energy principle yields an analytical relationship between the dimensionless fluid ejection frequency and the rate of energy loss which may be expressed in terms of the dimensionless shear stress

$$[16] \quad \frac{F_{ej}(h \cos\theta)}{V} \approx \frac{f}{5}$$

where F_{ej} is the average fluid ejection frequency. Equation [16] was derived for a wide chute with horizontal steps assuming that the ratio of average fluid ejection volume to total cavity volume is about 0.5 (Chanson and Toombes 2001*b*, pp. 56–58) and that the ratio of average ejection period to burst duration is about 7 (Djenidi et al. 1994; Tantirige et al. 1994). Note that, according to linear stability theory for a convective-type instability, a higher order cavity flow frequency is related to the flow momentum thickness and velocity (Lin and Rockwell 2001).

The result (eq. [16]) has practical applications in terms of fluid–structure interactions because cavity oscillations are the origin of coherent, broadband sources of noise and flow-induced vibrations. For example, if the natural frequency of the spillway structure is F_{ej}, major vibrations may occur, leading to potential damage and failure. Equation [16] suggests further that flow visualizations of cavity ejections and cavity pressure fluctuation measurements may provide some information on the flow resistance.

Interactions between the turbulent free-stream and unsteady recirculating flow are driven by the shear layer impingement process at the downstream end of the cavity (Fig. 1). In turn, the upstream flow conditions might affect self-excited cavity oscillations, inducing alterations of the mean drag (e.g., Lin and Rockwell 2001). Chanson and Toombes (2001*b*, pp. 36–38) suggested that different values of equivalent form drag friction factor might be related to different types of upstream flow conditions, i.e., $f = 0.105$, 0.17, and 0.30 in Fig. 4*c*.

Flow resistance on flat slopes

For flat slopes ($\theta < 20°$), the results highlight some discrepancies between the model and prototype data which remain unexplained (Fig. 4*a*). It must be noted, however, that the Brushes Clough spillway data (Baker 1994) were obtained for flow conditions characterized by Froude numbers close to unity ($Fr \approx 0.6$–1.2) and at the upper limit of the transition to skimming flow regimes (i.e., $d_c/h \approx 0.8$–1.0, where d_c is the critical flow depth). The Dneiper power plant data (Grinchuk et al. 1977) were obtained in decelerating flow conditions with Froude numbers slightly greater than unity ($Fr \approx 1.2$–4.0). In the laboratory, larger Froude numbers ($Fr \approx 3.3$–5.0) were observed. Although it is acknowledged that the prototype data might not be truly representative, these full-scale data exhibit some consistency between two series of experiments performed independently (i.e., Brushes Clough in the United Kingdom and Dneiper in the Ukraine).

In practice, it is believed that eq. [14*a*] is more representative of prototype flow conditions. The difference between eqs. [14*a*] and [14*b*] could suggest some form of scale effects. On a flat slope, the free surface is not parallel to the pseudo-bottom but exhibits an "undular" pattern in phase with the step geometry. The flow resistance is a combination of form drag and skin friction on the downstream end of each step. The interactions of the developing shear layer onto the downstream step cavity are significant, and the process may not be scaled properly with a Froude similitude. Further prototype flows were characterized by a larger Reynolds number and a larger relative channel width B/d than those of the model experiments. It is possible that the three-dimensional recirculation vortices were more intense, leading to larger flow-resistance data.

Flow resistance on steep slopes

For steep slopes ($\theta > 20°$), there is no skin friction between the main flow and the step faces, and the form drag associated with the recirculation predominates. The cavity flow is three dimensional, as observed during the present study, by Matos et al. (1999), and by A. Lejeune (personal communication) on the M'Bali Dam model. The flow resistance is a function of the recirculation process, and energy dissipation is dominated by the transfer of momentum between the cavity flow and the main stream. A simplified theoretical model (Appendix A) suggests that the pseudo-boundary shear stress form drag f_d may be expressed, in dimensionless form, as

$$[17] \quad f_d = \frac{2}{\sqrt{\pi}} \frac{1}{K}$$

where $1/K$ is the dimensionless rate of expansion of the shear layer (Fig. 1). In air–water mixing layers, Brattberg and Chanson (1998) observed $K \approx 6$ for $V = 2$–8 m/s. Equation [17] predicts that f_d is about 0.2 for a steep chute skimming flow which is close to the observed friction factor in skimming flow. Equation [17] is shown in Fig. 4*b*.

Fig. 5. Sketch of sequential fluid ejections in skimming flows.

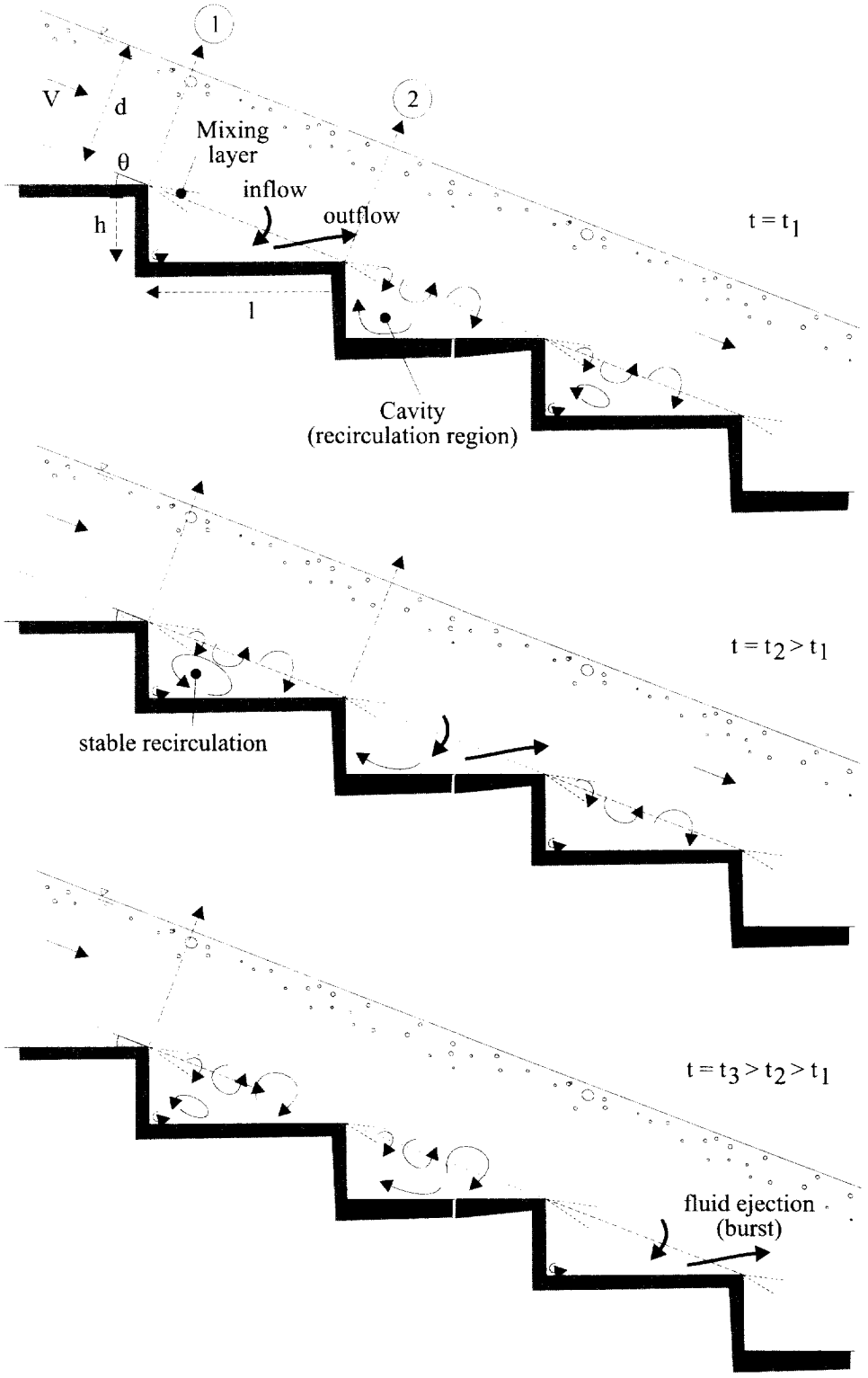

For steep slopes, the reasonable agreement between all the model data and the analytical development (eq. [17]) suggests that the analysis criteria (i.e., $h > 0.020$ m and $Re > 1 \times 10^5$) are satisfactory requirements for physical modelling of flow resistance in skimming flow based on a Froude similitude using a geometric similarity and the same fluids (air and water) in the model and the prototype. A further condition exists to achieve true similarity of air entrainment, i.e., a model scale between 1/1 and 1/10 (Kobus 1984; Chanson 1997).

In Fig. 4*b*, the flow-resistance data based on detailed air–water flow measurements appear centred around $f_e \approx 0.15$. The data, however, account for any drag reduction induced by free-surface aeration (Chanson 1993). For design pur-

poses, eq. [17] may provide a satisfactory estimate of the flow resistance, i.e., $f_e = f_d = 0.2$.

Final remarks

It is believed that channel width does affect the development and number of recirculating cells at each step. For steep chutes ($\theta > 20°$), data from Chamani and Rajaratnam (1999) and Yasuda and Ohtsu (1999) suggest slightly higher friction factors for low aspect ratios (i.e., $W/h \leq 10$) with identical flow conditions and geometry. Note that both studies used a constant channel breadth ($W = 0.3$ and 0.4 m, respectively), and the effect of channel width was not specifically investigated.

Lastly, flat slope prototype data exhibit greater friction factors than all model data, whereas laboratory data show flow-resistance estimates nearly independent of the slope.

Conclusions

In skimming flows down stepped chutes, the external edges of the steps form a pseudo-bottom over which the flow passes. Beneath this, recirculating vortices develop and are maintained through the transmission of shear stress from the waters flowing past the step edges. Skimming flows are characterized by a large flow resistance caused by form losses. The flow resistance is consistently larger than that on smooth-invert channels. Unsteady interactions between the recirculating cavities and the main stream are important. Flow visualizations suggest irregular fluid ejections from the cavity into the main stream, the process being sequential from upstream to downstream. On flat chutes ($\theta < 20°$), the flow resistance is a combination of skin friction on the horizontal faces of the steps and form drag associated with the recirculating cavity. The flow-resistance data may differ from steep chute data and may be correlated with the relative step roughness. Prototype results can be estimated using eq. [14*a*], but further work is required to understand the difference between model and prototype data.

On steep chutes ($\theta > 20°$), the flow resistance must be analysed as a form drag. It can be estimated from the maximum shear stress in the shear layers: eq. [17] presents a simple model of form loss that agrees well with steep chute data. Although they exhibit some scatter, the data are distributed around three dominant values ($f \approx 0.105$, 0.17, and 0.30). Air–water flow data show a smaller estimate $f_e \approx 0.15$, but the results may take into account some drag reduction induced by free-surface aeration. Physical modelling of flow resistance can be conducted based on a Froude similitude provided that the laboratory conditions satisfy $h > 0.020$ m and $Re > 1 \times 10^5$. To achieve true similarity of air entrainment, the model scale must be between 1/1 and 1/10.

The study emphasizes the complexity of skimming flow on stepped chutes, and the effects of free-surface aeration cannot be neglected. The flow resistance and energy dissipation processes are dominated by form losses and cavity recirculation.

Acknowledgments

The authors thank a large number of people for providing their experimental data, including Dr. R. Baker, University of Salford, U.K.; Dr. J. Matos, IST-Lisbon, Portugal; Mr. P. Royet, CEMAGREF; and Dr. L. Toombes, University of Queensland, Australia. The first author acknowledges the helpful discussion with Professor C.J. Apelt, University of Queensland, and Professor A. Lejeune, University of Liège, Belgium.

References

BaCaRa. 1991. Étude de la dissipation d'énergie sur les evacuateurs à marches. (Study of the energy dissipation on stepped spillways.) Report, Project National BaCaRa, CEMAGREF-SCP, Aix-en-Provence, France. (In French.)

Baker, R. 1994. Brushes Clough wedge block spillway: progress report no. 3. SCEL Project Report No. SJ542-4, University of Salford, Greater Manchester, U.K.

Bayat, H.O. 1991. Stepped spillway feasibility investigation. *In* Proceedings of the 17th International Commission on Large Dams (ICOLD) Congress, Vienna, Austria, Q66, R98, pp. 1803–1817.

Bindo, M., Gautier, J., and Lacroix, F. 1993. The stepped spillway of M'Bali Dam. International Water Power and Dam Construction, **45**(1): 35–36.

Boes, R.M. 2000. Zweiphasenstroömung und Energieumsetzung auf Grosskaskaden. Ph.D. thesis, VAW-ETH, Zürich, Switzerland. (In German.)

Brattberg, T., and Chanson, H. 1998. Air entrapment and air bubble dispersion at two-dimensional plunging water jets. Chemical Engineering Science, **53**(24): 4113–4127. Errata: 1999, **54**(12): 1925.

Chamani, M.R., and Rajaratnam, N. 1999. Characteristics of skimming flow over stepped spillways. ASCE Journal of Hydraulic Engineering, **125**(4): 361–368.

Chanson, H. 1993. Stepped spillway flows and air entrainment. Canadian Journal of Civil Engineering, **20**(3): 422–435.

Chanson, H. 1995. Hydraulic design of stepped cascades, channels, weirs and spillways. Pergamon, Oxford, U.K.

Chanson, H. 1997. Air bubble entrainment in free-surface turbulent shear flows. Academic Press, London, U.K.

Chanson, H. 1999. The hydraulics of open channel flows: an introduction. Edward Arnold, London, U.K.

Chanson, H. 2000. Forum article. Hydraulics of stepped spillways: current status. ASCE Journal of Hydraulic Engineering, **126**(9): 636–637.

Chanson, H., and Toombes, L. 2001*a*. Strong interactions between free-surface aeration and turbulence down a staircase channel. *In* Proceedings of the 14th Australasian Fluid Mechanics Conference, Adelaide, Australia, pp. 841–844.

Chanson, H., and Toombes, L. 2001*b*. Experimental investigations of air entrainment in transition and skimming flows down a stepped chute. Application to embankment overflow stepped spillways. Research Report No. CE 158, Department of Civil Engineering, The University of Queensland, Brisbane, Australia.

Chanson, H., Yasuda, Y., and Ohtsu, I. 2000. Flow resistance in skimming flow: a critical review. *In* Proceedings of the International Workshop on Hydraulics of Stepped Spillways, Zürich, Switzerland, 22–24 March 2000. *Edited by* H.-E. Minor and W.H. Hager. A.A. Balkema, Rotterdam, The Netherlands, pp. 95–102.

Christodoulou, G.C. 1993. Energy dissipation on stepped spillways. ASCE Journal of Hydraulic Engineering, **119**(5): 644–650. Discussion: **121**(10): 80–87.

Diez-Cascon, J., Blanco, J.L., Revilla, J., and Garcia, R. 1991. Studies on the hydraulic behaviour of stepped spillways. International Water Power and Dam Construction, **43**(9): 22–26.

Djenidi, L., Anselmet, F., and Antonia, R.A. 1994. LDA measurements in a turbulent boundary layer over a d-type rough wall. Experiments in Fluids, **16**: 323–329.

Elavarasan, R., Pearson, B.R., and Antonia, R.E. 1995. Visualization of near wall region in a turbulent boundary layer over transverse square cavities with different spacing. *In* Proceedings of the 12th Australasian Fluid Mechanics Conference AFMC, Sydney, Australia. *Edited by* R.W. Bilger. Vol. 1, pp. 485–488.

Frizell, K.H. 1992. Hydraulics of stepped spillways for RCC dams and dam rehabilitations. *In* Proceedings of the 3rd Specialty Conference on Roller Compacted Concrete, San Diego, California, 2–5 February 1992. *Edited by* K.D. Hansen and F.G. McLean. American Society of Civil Engineers, New York, pp. 423–439.

Goertler, H. 1942. Berechnung von Aufgaben der freien Turbulenz auf Grund eines neuen Näherungsansatzes. ZAMM, **22**: 244–254. (In German.)

Grinchuk, A.S., Pravdivets, Y.P., and Shekhtman, N.V. 1977. Test of earth slope revetments permitting flow of water at large specific discharges. Gidrotekhnicheskoe Stroitel'stvo, No. 4, pp. 22–26. (In Russian.) (Translated in Hydrotechnical Construction, **12**: 367–373.)

Haugen, H.L., and Dhanak, A.M. 1966. Momentum transfer in turbulent separated flow past a rectangular cavity. Journal of Applied Mechanics, Transactions ASME, September, pp. 641–464.

Henderson, F.M. 1966. Open channel flow. MacMillan Company, New York.

Kazemipour, A.K., and Apelt, C.J. 1983. Effects of irregularity of form on energy losses in open channel flow. Australian Civil Engineering Transactions, Vol. CE25, pp. 294–299.

Kistler, A.L., and Tan, F.C. 1967. Some properties of turbulent separated flows. Physics of Fluids. Part II, **10**(9): S165–S173.

Knauss, J. 1995. THS GRIAS TO PHDHMA, der Altweibersprung. Die Rätselhafte Alte Talsperre in der Glosses-Schlucht bei Alyzeia in Akarnanien. Archäologischer Anzeiger, **5**: 138–162. (In German.)

Kobus, H. (*Editor*). 1984. Proceedings of the International Association for Hydraulic Research Symposium on Scale Effects in Modelling Hydraulic Structures, Esslingen, Germany, 3–6 September 1984. Technische Akademie Esslingen, Ostfildern, Germany.

Lin, J.C., and Rockwell, D. 2001. Organized oscillations of initially turbulent flow past a cavity. AIAA Journal, **39**(6): 1139–1151.

Matos, J. 2000. Hydraulic design of stepped spillways over RCC dams. *In* Proceedings of the International Workshop on Hydraulics of Stepped Spillways, Zürich, Switzerland, 22–24 March 2000. *Edited by* H.-E. Minor and W.H. Hager. A.A. Balkema, Rotterdam, The Netherlands, pp. 187–194.

Matos, J., Sanchez, M., Quintela, A., and Dolz, J. 1999. Characteristic depth and pressure profiles in skimming flow over stepped spillways. *In* Proceedings of the 28th Biennial Congress of the International Association for Hydraulic Research, Graz, Austria, 22–27 August 1999, Session B14. CD-ROM.

Ohtsu, I., and Yasuda, Y. 1997. Characteristics of flow conditions on stepped channels. *In* Proceedings of the 27th Biennial Congress of the International Association for Hydraulic Research, San Francisco, California, 10–15 August 1997. *Edited by* F.M. Holly Jr. and A. Alsaffar. Thomas Telford, London, Theme D, pp. 583–588.

Ohtsu, I., and Yasuda, Y. (*Editors*). 1998. Hydraulic Characteristics of Stepped Channel Flows, Proceedings of the Workshop on Flow Characteristics Around Hydraulic Structures and River Environment. University Research Center, Nihon University, Tokyo, Japan.

Ohtsu, I., Yasuda, Y., and Takahashi, M. 2000. Characteristics of skimming flow over stepped spillways. Discussion. ASCE Journal of Hydraulic Engineering, **126**(11): 869–871.

Pearson, B.R., Elavarasan, R., and Antonia, R.A. 1997. The response of a turbulent boundary layer to a square groove. Journal of Fluids Engineering, Transactions of ASME, **119**: 466–469.

Peyras, L., Royet, P., and Degoutte, G. 1991. Ecoulement et dissipation sur les déversoirs en gradins de gabions. (Flows and dissipation of energy on gabion weirs.) Journal la Houille Blanche, No. 1, pp. 37–47. (In French.)

Ruff, J.F., and Frizell, K.H. 1994. Air concentration measurements in highly-turbulent flow on a steeply-sloping chute. *In* Proceedings of the ASCE Hydraulic Engineering Conference, Buffalo, N.Y., 1–5 August 1994. *Edited by* C.A. Pugh. American Society of Civil Engineers, New York, Vol. 2, pp. 999–1003.

Schlichting, H. 1979. Boundary layer theory. 7th ed. McGraw-Hill, New York.

Shvajnshtein, A.M. 1999. Stepped spillways and energy dissipation. Gidrotekhnicheskoe Stroitel'stvo, No. 5, pp. 15–21. (In Russian.) Also in Hydrotechnical Construction, **3**(5): 275–282.

Sorensen, R.M. 1985. Stepped spillway hydraulic model investigation. ASCE Journal of Hydraulic Engineering, **111**(12): 1461–1472. Discussion: **113**(8): 1095–1097.

Tantirige, S.C., Iribarne, A.P., Ojhas, M., and Trass, O. 1994. The turbulent boundary layer over single V-shaped cavities. International Journal of Heat and Mass Transfer, **37**: 2261–2271.

Tozzi, M., Taniguchi, E., and Ota, J. 1998. Air concentration in flows over stepped spillways. *In* FEDSM'98, Proceedings of the 1998 ASME Fluids Engineering Conference, Washington, D.C., 21–25 June 1998. Paper FEDSM98-5053. CD-ROM.

Wygnanski, I., and Fiedler, H.E. 1970. The two-dimensional mixing region. Journal of Fluid Mechanics, Part 2, **41**: 327–361.

Yasuda, Y., and Ohtsu, I. 1999. Flow resistance of skimming flow in stepped channels. *In* Proceedings of the 28th Biennial Congress of the International Association for Hydraulic Research, Graz, Austria, 22–27 August 1999, Session B14. CD-ROM.

List of symbols

A_w cross-sectional area (m^2) of the water flow

C air concentration, defined as the volume of air per unit volume (also called void fraction)

C_{mean} depth-averaged air concentration, defined as $(1 - Y_{90})C_{mean} = d$

C_P pressure correction coefficient

D_H hydraulic diameter (m)

D' dimensionless air bubble diffusivity

d flow depth measured normal to the channel slope at the edge of a step; characteristic depth (m) defined as $d = \int_0^{Y_{90}} (1 - C)\, dy$

d_c critical flow depth

d_1 flow depth (m) upstream of a hydraulic jump

d_2 flow depth (m) downstream of a hydraulic jump

f Darcy friction factor

f_d (equivalent) Darcy friction factor estimate of the form drag

f_e Darcy friction factor for air–water flow

f_p Darcy friction factor calculated using eq. [13]

f_w Darcy friction factor for clear-water (non-aerated) flow

F_{ej} average fluid ejection frequency (Hz)

Fr Froude number, defined as $Fr = V/\sqrt{gd}$

g gravity constant (m/s^2) or acceleration of gravity

h height of steps (m) (measured vertically)

H total head (m)
H_{res} residual head (m) at the downstream end of the chute
k_s step dimension (m) measured normal to the flow direction ($k_s = h \cos \alpha$)
k_s' surface (skin) roughness height (m)
K inverse of the spreading rate of a turbulent shear layer
K' integration constant (defined by Chanson 1997)
l horizontal length of steps (m) (measured perpendicular to the vertical direction)
P pressure (Pa)
P_{bottom} invert pressure (Pa)
P_w wetted perimeter (m)
q discharge per unit width (m^2/s)
q_w water discharge per unit width (m^2/s)
Q_w water discharge (m^3/s)
Re Reynolds number, defined as $Re = VD_H/\nu_w$
S_f friction slope, defined as $S_f = -\partial H/\partial x$
t time (s)
t_1, t_2, t_3 times (s)
v local velocity (m/s)
V clear-water flow velocity (m/s), defined as $V = q_w/d = q_w / \int_0^{Y_{90}} (1 - C)\, dy$
V_0 free-stream velocity (m/s)
V_1 flow velocity (m/s) upstream of a hydraulic jump
V_2 flow velocity (m/s) downstream of a hydraulic jump
W channel width (m)
x longitudinal distance (m) measured in the flow direction
y distance (m) from the pseudo-bottom (formed by the step edges) measured perpendicular to the flow direction
y_{50} distance (m) normal to the invert where $V = V_0/2$
Y_{90} characteristic depth (m) where the air concentration is 90%
μ dynamic viscosity ($N \cdot s/m^2$)
ν kinematic viscosity (m^2/s)
ν_t turbulent kinematic viscosity (m^2/s)
ρ density (kg/m^3)
σ surface tension between air and water (N/m)
τ shear stress (Pa)
τ_{max} maximum shear stress (Pa) in a shear layer
τ_o average bottom shear stress (Pa)
θ channel slope

Subscripts

c critical flow conditions
w water flow

Appendix A. Modelling form drag and flow resistance in skimming flows

Skimming flows are characterized by unsteady momentum exchanges between the main stream and cavity flows. For a steep slope ($\theta > 20°$), the form drag associated with the recirculation is preponderant. The cavity flow is three-dimensional as visually observed by A. Lejeune (personal communication) on the M'Bali Dam model and during the present study. The flow resistance is a function of the recirculation process, and energy dissipation is dominated by the transfer of momentum between the cavity flow and the main stream.

Estimating the boundary shear stress along a recirculating cavity

At each step, the cavity flow is driven by the developing shear layer and the transfer of momentum across it (Fig. 1). The mixing layer is basically a free shear layer. The equivalent boundary shear stress of the cavity flow equals the maximum shear stress in the shear layer that may be modelled by a mixing length model

$$[A1] \quad \frac{\nu}{V_o} = \frac{1}{2}\left\{1 + \text{erf}\left[\frac{K(y - y_{50})}{x}\right]\right\}$$

assuming a constant eddy viscosity ν_t across the shear layer

$$[A2] \quad \nu_t = \frac{1}{4K^2} x V_o$$

where $1/K$ is the dimensionless rate of expansion of the shear layer, y_{50} is the location of the streamline $v = V_o/2$, and V_o is the free-stream velocity (Goertler 1942). The boundary shear stress between the outer flow and the cavity flow equals the maximum shear stress in the mixing layer

$$[A3] \quad \tau_o = \tau_{max} = \rho \nu_t \left(\frac{\partial v}{\partial y}\right)_{y = y_{50}}$$

where ν_t is the momentum exchange coefficient (eq. [A2]). For the approximation of Goertler (1942), the dimensionless pseudo-boundary shear stress equals

$$[A4] \quad f_d = \frac{8\tau_{max}}{\rho V_o^2} = \frac{2}{\sqrt{\pi} K}$$

where the term on the left-hand side is basically a pseudo Darcy friction factor (Chanson et al. 2000).

In air–water mixing layers of plane plunging jets, Brattberg and Chanson (1998) observed $K \approx 6$ for velocities ranging from 2 to 8 m/s. (For monophase flows, $K \approx 12$.). Equation [A4] predicts a form drag $f_d \approx 0.2$ for skimming flow, a result close to friction factor data in steep stepped flows. In monophase flows, Wygnanski and Fiedler (1970) observed that the maximum shear stress is independent of the distance from the singularity, and their data yield $f = 0.18$. For cavity flows, Haugen and Dhanak (1966) and Kistler and Tan (1967) observed similar results.

Discussion

It must be emphasized that the development in the previous section (i.e., eq. [A4]) does not take into account the interactions between the developing mixing layer and the downstream step and the associated losses. Pearson et al. (1997) demonstrated that turbulent flows past a recirculating square cavity are associated with a sharp rise of boundary shear stress downstream of the cavity for up to six cavity lengths. Their data showed the magnitude of the shear stress peak being about three times the equivalent skin friction stress. Pearson et al. attributed the sharp rise to a local intense favourable pressure gradient that is associated with the downstream stagnation edge of the cavity. This is in fact a kind of form drag.